



Check for updates

Condensed Matter Physics. Physics of Low-Dimensional Structures and Nanostructures

UDC 548.4

<https://www.doi.org/10.33910/2687-153X-2021-2-2-51-60>

A model of strain hardening in nanoceramics with amorphous intercrystalline layers

M. Yu. Gutkin^{✉1}, K. N. Mikaelyan¹

¹ Institute for Problems in Mechanical Engineering of the Russian Academy of Sciences, 61 Bolshoy Ave., Saint Petersburg 199178, Russia

Authors

Mikhail Yu. Gutkin, ORCID: 0000-0003-0727-6352, e-mail: m.y.gutkin@gmail.com

Kristina N. Mikaelyan, e-mail: kristy_mik@gmail.com

For citation: Gutkin, M. Yu., Mikaelyan, K. N. (2021) A model of strain hardening in nanoceramics with amorphous intercrystalline layers. *Physics of Complex Systems*, 2 (2), 51–60. <https://www.doi.org/10.33910/2687-153X-2021-2-2-51-60>

Received 17 March 2021; reviewed 30 March 2021; accepted 30 March 2021.

Copyright: © The Authors (2021). Published by Herzen State Pedagogical University of Russia. Open access under [CC BY-NC License 4.0](https://creativecommons.org/licenses/by-nc/4.0/).

Abstract. The article suggests a theoretical model which describes the development of plastic deformation within amorphous intercrystalline layers in nanocrystalline ceramics as a process of homogeneous generation of inclusions of the liquid-like phase, their extension and further penetration to neighbouring layers through triple junctions. The energetic characteristics of these stages are calculated and analysed in detail. It is shown that the nucleation stage can be realised in the barrier-less regime when the applied shear stress reaches its critical value which depends on the temperature of the mechanical testing. The penetration stage of the deformation process needs some increase in the applied shear stress and, therefore, leads to strain hardening of the model nanocrystalline ceramics. The corresponding flow stress increases with diminishing grain size of the nanoceramics and lowering temperature of testing.

Keywords: nanocrystalline ceramics, amorphous intercrystalline layers, inclusions, liquid-like phase, plastic deformation, strain hardening.

Introduction

It is well known that in certain ceramics with covalent chemical bonding like Al_2O_3 , SiC , Si_3N_4 , SrTiO_3 , etc., the grain boundaries (GBs) can contain amorphous films of about 1–2 nm thickness, which are also called ‘intergranular glassy films’ (IGFs). Earlier research by D. R. Clarke was aimed at the detection of IGFs with electron microscopy (Clarke 1979) and explanation of their existence and stability (Clarke 1987). Many experimental observations were made by Rühle’s group (see, for example, Kleebe et al. 1992; 1993). These and other related results on IGFs in ceramics and ceramic matrix composites are presented in collective monographs (Dufour et al. 1989; Hoffmann, Petzow 1994; Tomsia, Glaeser 1998) and reviews (Kleebe 1997; Subramaniam et al. 2006). In particular, it was shown that IGFs have a nearly constant thickness which is basically independent of the orientation of the bounding grains, but is dependent on the composition of ceramics (Subramaniam et al. 2006). The presence of IGFs can play an important role in determining the properties of ceramics as a whole, such as strength, toughness, fatigue, etc. (Hoffmann, Petzow 1994; Chen et al. 2000). It is worth noting that IGFs in ceramic silicon nitride attract special attention of many researchers (Clarke 1979; 1987; Hoffmann, Petzow 1994; Kleebe et al. 1992; 1993; Zhang et al. 2011).

Extensive investigations in the field of nanocrystalline materials have stimulated the interest in IGFs in nanocrystalline ceramics (Keblinski et al. 1996; 1997; Mo, Szlufarska 2007; Szlufarska et al. 2005) in relation to their outstanding mechanical properties (Hulbert et al. 2007; Xu et al. 2006). Since the experimental observations in this field are extremely complicated and laborious, a significant role

is played by computer simulations (Demkowicz et al. 2007; Demkowicz, Argon 2004; 2005a; 2005b; Koblinski et al. 1996; 1997; Mo, Szlufarska 2007; Szlufarska et al. 2005) and analytical theoretical models (Bobylev et al. 2008; Bobylev, Ovid'ko 2008; Glezer, Pozdnyakov 1995; Gutkin, Ovid'ko 2009; 2010a; 2010b; Ovid'ko et al. 2008; Pozdnyakov, Glezer 1995). Thus, computer simulation results give a basis for developing theoretical analytical models which, in their turn, show directions for further computer simulations.

In particular, researchers (Demkowicz, Argon 2004; 2005a; 2005b) simulated bulk amorphous silicon (a-Si) as a typical amorphous covalent material and showed that its atomic structure includes liquid-like and solid-like regions. The volume fractions of these components depend on the cooling rate of liquid silicon, which leads to a change in the plastic flow regime of the simulated samples—the higher the volume fraction of the liquid-like material is, the more homogeneous the plastic flow of a-Si is. Moreover, the fraction of the liquid-like phase increases under mechanical loading. The authors concluded that the liquid-like phase regions are the carriers of plastic deformation in a-Si. Since the latter is a typical example of an amorphous covalent material, they suggested that these features are also inherent in other amorphous solids with covalent bonding, in particular, in GB layers of amorphous silicon nitride (a-Si₃N₄) surrounding the titanium nitride nanograins (nc-TiN) in nc-TiN/a-Si₃N₄ ceramic nanocomposite. Later, the formation and growth of the liquid-like phase regions in the GBs were observed in a computer simulation of the plastic deformation of nc-Si (Demkowicz et al. 2007).

Based on the results of the computer simulations (Demkowicz, Argon 2004; 2005a; 2005b; Demkowicz et al. 2007), a theoretical model of the plastic deformation of an amorphous covalent material was suggested in (Gutkin, Ovid'ko 2009; 2010a) and later used for the description of the mechanical behaviour of amorphous intercrystalline layers in nanoceramics (Gutkin, Ovid'ko 2009; 2010b). This model describes the following main features of the plastic deformation of amorphous covalent material (Gutkin, Ovid'ko 2010a):

- (1) The mechanism of plastic deformation is the homogeneous nucleation and development of liquid-like phase inclusions under the applied shear stress.
- (2) Such inclusions exhibit a plastic shear modelled by glide dislocation loops, which appear and develop simultaneously with the inclusions.
- (3) The formation of such inclusions does not require overcoming the energy barrier if the applied stress reaches some critical temperature-dependent level; the higher the temperature is, the lower the critical stress is.
- (4) In the case of the barrierless nucleation of the inclusion at relatively low temperatures, the strength (the Burgers vector) of the dislocation loop, which models the plastic shear inside the inclusion, increases faster than the loop size. In this case, the heterogeneous plastic flow of the amorphous material due to the concentration of the plastic deformation in narrow slip bands should be expected.
- (5) If the barrierless nucleation of the inclusion proceeds at a relatively high temperature, an increase in the size of the dislocation loop advances an increase in its strength and a homogeneous plastic flow of the material via the bulk nucleation and gradual development of such inclusions should be expected. If, in addition, the applied stress exceeds the critical level for the barrierless nucleation of inclusions, the transition from the homogeneous to heterogeneous flow of the amorphous material becomes possible.

For a model case of nc-TiN/a-Si₃N₄ ceramic nanocomposite, the papers (Gutkin, Ovid'ko 2009; 2010b) show that, when the length of the amorphous layer is large enough and a considerable dislocation charge is accumulated, the inclusions of the liquid-like phase induce the formation and growth of mode I–II cracks in neighbouring amorphous layers. In this case, the possibility of opening and growing the crack depends very strongly on the test temperature, the layer orientation, and the size of nanoceramic grains. An increase in the temperature and the angle of orientation and a decrease in the size of nanoceramic grains favour an increase in the crack resistance.

In the present paper, we consider another scenario of the plastic deformation development when the crack opening is suppressed. In this case, it is assumed that the inclusion of the liquid-like phase can overcome the triple junction of amorphous intercrystalline layers and penetrate into one of the neighbouring layers. We show that this process needs some increase in the applied shear stress and, therefore, leads to strain hardening of model nanocrystalline ceramics.

Model

According to the approach proposed in (Gutkin, Ovid'ko 2009; 2010a), we consider a model nanoceramic sample, to which a normal tensile stress σ is applied, and one of the amorphous intergranular interlayers of length L and thickness h , in which the maximum shear stress $\tau = \sigma/2$ acts (Fig. 1). Based on the results (Gutkin, Ovid'ko 2009; 2010a), we assume that until this stress reaches a certain critical value $\tau = \tau_c$, the sample is elastically deformed. Upon reaching the critical stress τ_c , which corresponds to the critical elastic shear deformation $\varepsilon_c = \tau_c/(2G)$, where G is the shear modulus, a nucleus of a liquid-like phase with plastic shear localised in it is formed in the amorphous interlayer without any energy barrier. For the sake of simplicity, the local plastic shear is modelled here by a dipole of edge dislocations with variable Burgers vectors $\pm s$. Under the action of stress $\tau \geq \tau_c$, the longitudinal size p of the nucleus grows and reaches the length of the amorphous interlayer L . At the same time, the magnitude s of the Burgers vector also increases. As shown by the calculations (Gutkin, Ovid'ko 2009; 2010a), the value of s in the first approximation is directly proportional to the size of the nucleus p : $s \approx \eta p$, $\eta < 1$. At relatively low temperatures of the deformation test, the calculations (Gutkin, Ovid'ko 2009; 2010a) show $\eta \approx 0.2$, while at relatively high temperatures they show $\eta \approx 0.05$.

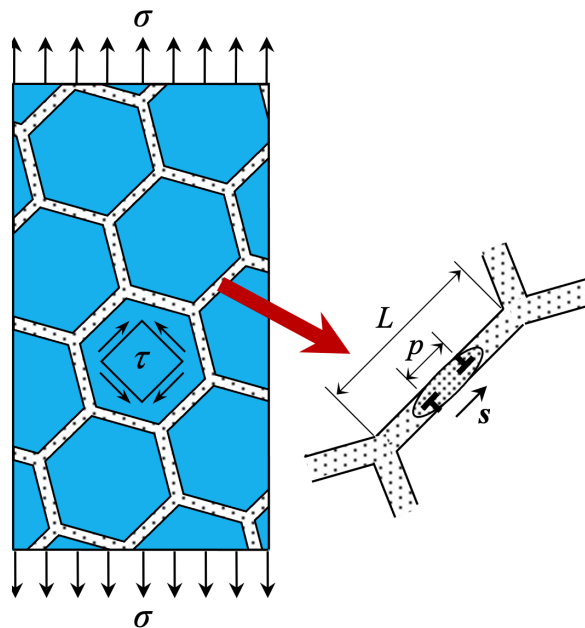


Fig. 1. A two-dimensional model of the plastic flow of nanoceramics due to the formation of nuclei of the liquid-like phase in the grain boundaries in which plastic shear develops, simulated by a dipole of edge dislocations with a growing Burgers vector s

Let us use this model to calculate stress-strain curves for such a model nanoceramic sample. The plastic deformation of the sample can be estimated with the following formula (Ovid'ko, Sheinerman 2009):

$$\varepsilon \approx \alpha \frac{s}{d} \approx \alpha \eta \frac{p}{d}, \tag{1}$$

where α is the fraction of grain boundaries oriented in such a way that a given stress τ acts in them (Ovid'ko, Sheinerman 2009), and d is the average grain size of the sample.

The formation and growth of one nucleus of a liquid-like phase in a grain boundary with a suitable orientation in nanoceramics is accompanied by a change in the energy of the system (per unit dislocation length) by the value

$$\Delta W = W_d + HS - \tau sp, \tag{2}$$

where W_d is the strain energy of the dislocation dipole, H is the excess enthalpy of the liquid-like phase in comparison with the solid-like phase, and S is the cross-sectional area of the nucleus of the liquid-like

phase. Assuming that the arm of the dipole is approximately equal to the longitudinal size of the nucleus p , we can write the strain energy W_d as follows (Gutkin, Ovid'ko, Skiba 2004):

$$W_d = \frac{Gs^2}{2\pi(1-\nu)} \ln \frac{p-r_c}{r_c} \approx \frac{G\eta^2 p^2}{2\pi(1-\nu)} \ln \frac{1-\eta}{\eta}, \quad (3)$$

where ν is the Poisson ratio, $rc \approx s \approx \eta\rho$ is the cutoff radius of the elastic field of the dipole at the dislocation lines. For simplicity, we will assume that $S = pt \approx p\xi b$, where t is the transverse size of the nucleus, $\xi \approx 2...4$, and b is the average interatomic distance.

With Eq. (3) and the assumptions made, Eq. (2) takes the following form:

$$\Delta W = \frac{G\eta^2 p^2}{2\pi(1-\nu)} \ln \frac{1-\eta}{\eta} + H\xi bp - \tau\eta p^2. \quad (4)$$

Results

In the numerical investigation of the energy change ΔW , we used the material characteristics for nanoceramic silicon nitride (Si_3N_4) as was the case in (Gutkin, Ovid'ko 2009; 2010b): $G = 120 \text{ GPa}$, $\nu = 0.2$, and $b \approx 0.174 \text{ nm}$; at relatively low temperatures of testing, we took $H = 0.05 \text{ eV/at.}$ and $n \approx 0.2$, while at relatively high temperatures of testing, $H = 0.01 \text{ eV/at.}$ and $n \approx 0.05$. For the sake of definiteness, it was also assumed that $\xi \approx 2$.

Fig. 2 shows the dependences $\Delta W(p)$ plotted at different values of the applied shear stress τ for relatively (a) low and (b) high temperatures. It is seen that, depending on the level of τ , the curves $\Delta W(p)$ can demonstrate rather different behaviours. They can monotonously increase at relatively low values of τ , or first increase, reach their maxima and then decrease at some intermediate values of τ , or monotonously decrease at relatively high values of τ . In the first case, the formation of the liquid-like phase nucleus is energetically unfavourable and, therefore, impossible. In the second and third cases, the nucleus formation is possible if the corresponding energy barrier is either small enough or even absent.

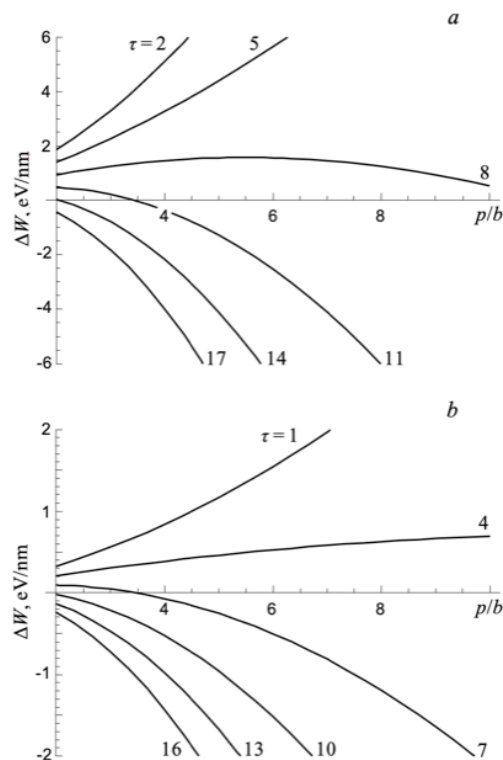


Fig. 2. Dependence of the energy change ΔW on the normalised size p/b of the nucleus of the liquid-like phase for different values of the applied shear stress τ (in units of GPa) at (a) low and (b) high temperatures

The most strict and reliable conditions for the nucleus formation event are that (i) the energy change ΔW is not positive for some initial nucleus size, and (ii) the energy change ΔW monotonously decreases with the nucleus size p . It is seen from the plots shown in Fig. 2 that these conditions are satisfied if τ reaches a critical value, $\tau = \tau_c(T)$. At relatively low temperatures, $\tau_c \approx 14 \text{ GPa}$, while at relatively high temperatures, $\tau_c \approx 9.5 \text{ GPa}$.

It also follows from these plots that at stress values equal to or higher than the critical one, the nucleus of the liquid-like phase develops in an unstable regime. Obviously, this happens until it reaches the nearest obstacle, which, in the case of nanoceramics, is the nearest triple junction of grain boundaries. Overcoming the triple junction leads to a displacement of the boundary that is not subjected to the shear (Fig. 3) and to the formation (in the case of tilt boundaries) of a dipole of partial wedge disclinations of strength ω equal to the misorientation angle of this boundary and with an arm equal to the displacement of the boundary (Ovid'ko, Sheinerman 2009). A further increase in the size of the nucleus of the liquid-like phase, accompanied by an increase in the plastic shear, causes an elongation of the disclination dipole arm and a corresponding increase in its energy, hence the appearance of a thermodynamic force that prevents the propagation of the liquid-like phase. To overcome this force, it is necessary to further increase the applied stress level. Thus, the transition of the system to the hardening stage should be expected.

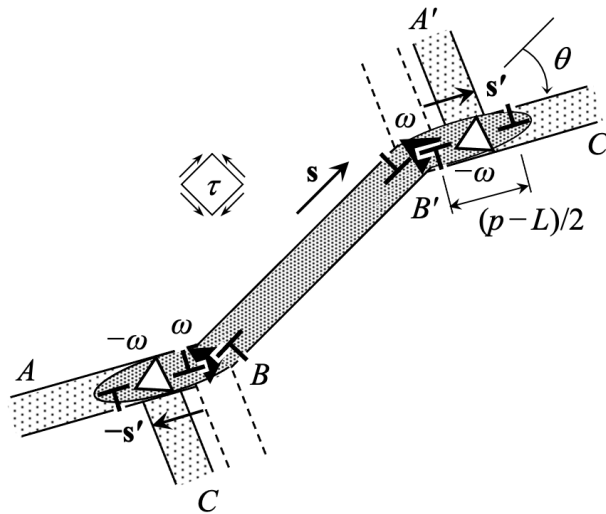


Fig. 3. Model of nucleation of the secondary nuclei of the liquid-like phase along the grain boundaries AB and B'C'. The development of the secondary nuclei of the liquid-like phase is accompanied by their plastic shear, which is modelled by two new dipoles of edge dislocations with arms $(p - L)/2$ and Burgers vectors $\pm s'$. The plastic shears are accompanied by the displacements of the grain boundaries A'B' and BC by vectors s' and $-s'$, respectively, and the appearance of two dipoles of partial wedge disclinations with arms s' and strengths $\pm \omega$

To calculate the stress providing plastic deformation at the hardening stage, consider the model shown in Fig. 3. It shows the grain boundary BB' filled with the liquid-like phase and subjected to plastic shear. This plastic shear is modelled by a dipole of edge dislocations pressed by the applied stress $\tau \geq \tau_c$ to two triple junctions B and B', on which secondary nuclei of the liquid-like phase are generated along the neighbouring boundaries AB and B'C'. The development of these secondary nuclei of the liquid-like phase is accompanied by their plastic shear, which is modelled by two new dipoles of edge dislocations with the Burgers vector $\pm s'$, the magnitude of which increases with an increase in the size of these nuclei $s' \approx \eta(p-L)/2$, where p is the total length of the liquid-like phase ABB'C' and L is the length of the boundary BB'. At the same time, the boundaries BC and A'B' are displaced in opposite directions by distances s' with the formation of two biaxial dipoles of partial wedge disclinations with arms s' . For simplicity of further calculations, we assume that the strengths of these dipoles are the same and equal to ω .

The change in the energy of the system $\Delta W'$ accompanying the formation of two secondary nuclei of the liquid-like phase (Fig. 3) can be written in the following form:

$$\Delta W' = 2W'_d + W_{qd} + W_{d,int} + H\xi b(p - L) - \tau \cos(2\theta) s' (p - L), \quad (5)$$

where $2W'_d$ is the self-strain energy of two new dislocation dipoles, W_{qd} is the self-strain energy of the disclination quadrupole, $W_{d,int}$ is the energy of the elastic interaction of the new dislocation dipoles with the old one, θ is the angle of deviation of the boundaries AB and B'C' from the straight line BB'. Note that in the first approximation we neglect the elastic interaction of new dislocation dipoles with each other and with the 'opposite' disclination dipoles. If necessary, these terms can be taken into account, although they are unlikely to be significant.

We write the first term in Eq. (5) by analogy with Eq. (3) as follows:

$$2W'_d = \frac{2Gs'^2}{2\pi(1-\nu)} \ln \frac{(p-L)/2-r_c}{r_c} \approx \frac{G\eta^2(p-L)^2}{4\pi(1-\nu)} \ln \frac{1-\eta}{\eta}. \quad (6)$$

The second term of Eq. (5) is approximated by the well-known expression for a disclination quadrupole in which all disclinations lie on the same line (Romanov, Vladimirov 1992). Substituting our definition of the dipole arm into this expression, after some algebra we have

$$W_{qd} = \frac{G\omega^2\eta^2(p-L)^2}{16\pi(1-\nu)} \left\{ \ln \frac{4L[L+\eta(p-L)]}{\eta^2(p-L)^2} + \left(\frac{2L+\eta(p-L)}{\eta(p-L)} \right)^2 \ln \frac{4L[L+\eta(p-L)]}{[2L+\eta(p-L)]^2} \right. \\ \left. + 2 \frac{2L+\eta(p-L)}{\eta(p-L)} \ln \frac{L+\eta(p-L)}{L} \right\}. \quad (7)$$

The third term in Eq. (5) was calculated in (Gutkin, Ovid'ko, Pande 2004). With our denotations, it takes the following form:

$$W_{d,int} = -\frac{G\eta^2(p-L)L}{2\pi(1-\nu)} \left\{ \frac{\cos\theta}{2} \ln \frac{4L^2}{\eta^2[4L^2 + 4L(p-L)\cos\theta + (p-L)^2]} \right. \\ \left. + \frac{2L(p-L)\sin^2\theta}{4L^2 + 4L(p-L)\cos\theta + (p-L)^2} \right\}. \quad (8)$$

Thus, all terms of Eq. (5) are defined. Fig. 4 shows the dependence of the energy change $\Delta W'$ on the normalised size p/b of the nucleus of the liquid-like phase for $L = 100b$, $\omega = \pi/3$, $\theta = \pi/6$, and different values of the applied shear stress τ at (a) low and (b) high temperatures. The upper curves are plotted for the corresponding values of the critical stress $\tau_c = 14$ and 9.5 GPa. It is seen that even at these values, it is energetically favourable for new critical nuclei to grow to significant sizes of the order of $25b \approx 4.35$ nm at low temperatures and up to $65b \approx 11.31$ nm at high temperatures. However, their further growth requires an increase in the level of τ .

In the case of quasi-static loading, we can assume (Ovid'ko, Sheinerman 2009) that each level of the stress $\tau \geq \tau_c$ will correspond to the equilibrium size of the nucleus of the liquid-like phase and, accordingly, the magnitude of plastic shear. The equilibrium condition is determined by the equation $\partial\Delta W'(p)/\partial p = 0$, from which we immediately find

$$\tau = \frac{G\eta}{4\pi(1-\nu)\cos 2\theta} \left\{ 2 \ln \frac{1-\eta}{\eta} - \frac{L\cos\theta}{p-L} \ln \frac{4L^2}{\eta^2[4L^2 + 4L(p-L)\cos\theta + (p-L)^2]} \right. \\ \left. - \frac{16L^3\sin^2\theta[2L+(p-L)\cos\theta]}{[4L^2 + 4L(p-L)\cos\theta + (p-L)^2]^2} + \frac{2L\cos\theta(2L\cos\theta + p-L)}{4L^2 + 4L(p-L)\cos\theta + (p-L)^2} \right. \\ \left. + \omega^2 \left[\ln \frac{2L+2\eta(p-L)}{\eta(p-L)} + \frac{2L+\eta(p-L)}{\eta(p-L)} \ln \frac{2L+2\eta(p-L)}{2L+\eta(p-L)} \right] \right\} + \frac{H\xi b}{\eta(p-L)\cos 2\theta}. \quad (9)$$

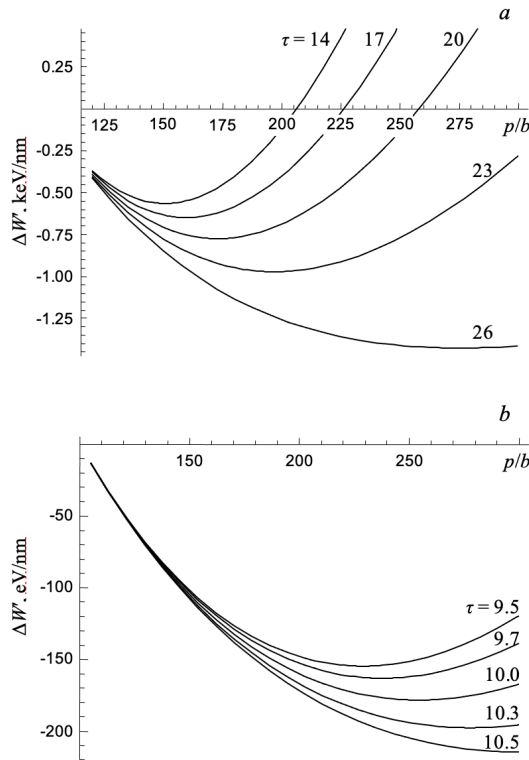


Fig. 4. Dependence of the energy change $\Delta W'$ on the normalised size p/b of the nucleus of the liquid-like phase for different values of the applied shear stress τ (in units of GPa) at (a) low and (b) high temperatures.

Let us now find the plastic deformation occurring in the plane of the grain boundary BB' . It can be estimated by the sum

$$\varepsilon = \varepsilon_1 + \varepsilon_2, \tag{10}$$

where ε_1 is the plastic deformation due to the shear inside the primary nucleus of the liquid-like phase, which is determined by formula (1) at $p = L$:

$$\varepsilon_1 \approx \alpha\eta \frac{L}{d}, \tag{11}$$

and ε_2 is the plastic deformation due to the shear inside the secondary nuclei of the liquid-like phase, which, by analogy, can be written as

$$\varepsilon_2 \approx \alpha\eta \frac{(p-L)\cos\theta}{2d}. \tag{12}$$

Then it follows from Eq. (10) with Eqs. (11) and (12) that

$$p - L \approx \frac{2}{\cos\theta} \left(\frac{\varepsilon d}{\alpha\eta} - L \right). \tag{13}$$

Now, assuming that $d \approx 1.5L$, we can make the substitution $p - L \approx L[3\varepsilon/(\alpha\eta) - 2]/\cos\theta$ in Eq. (9), which gives the dependence $\tau(\varepsilon)$.

Fig. 5 shows the curves $\tau(\varepsilon)$ plotted for different values of the grain boundary length L at relatively (a) low and (b) high temperatures. It is seen that grain refinement (shortening of grain boundaries) of nanoceramics leads to some increase in the flow stress.

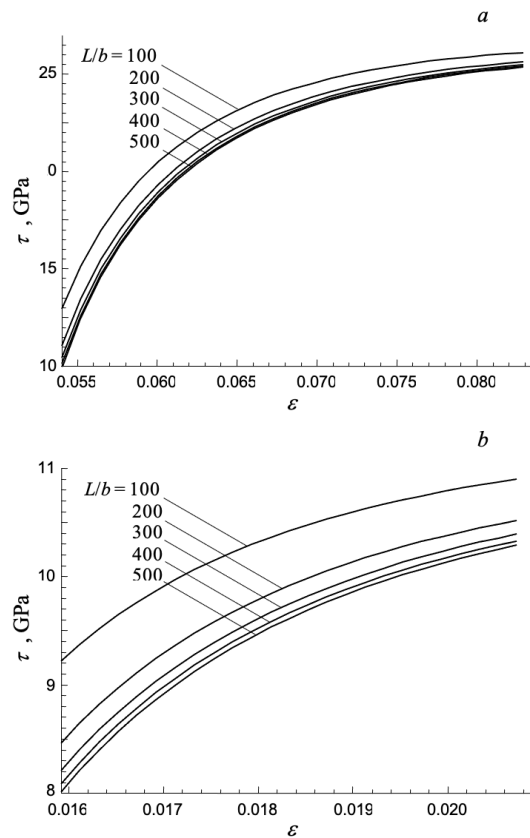


Fig. 5. Dependence of the shear stress on the plastic deformation at the stage of hardening of Si_3N_4 nanoceramics for different lengths L of the grain boundaries at relatively (a) low and (b) high temperatures

Thus, we have considered the case of penetration of an inclusion of the liquid-like phase from one amorphous intercrystalline layer to another through a triple junction of such layers, which is alternative to the case of the crack opening at the triple junction studied in (Gutkin, Ovid'ko 2009; 2010b). We have shown that this process needs some increase in the applied shear stress and, therefore, leads to strain hardening of the model nanoceramics. The corresponding flow stress increases with diminishing grain size of the nanoceramics and is higher for low temperatures than for high temperatures.

Conclusion

In summary, the study suggests a theoretical model which describes the development of plastic deformation within amorphous intercrystalline layers in nanocrystalline ceramics as a process of homogeneous generation of inclusions of the liquid-like phase, their extension and further penetration to neighbouring layers through their triple junctions. The energetic characteristics of these stages are calculated and analysed in detail.

It is shown that the nucleation stage can be realised in the barrier-less regime when the applied shear stress reaches its critical value which depends on the temperature of the mechanical testing. The higher the temperature is, the smaller the critical stress is.

The penetration stage of the deformation process needs some increase in the applied shear stress and, therefore, leads to strain hardening of model nanocrystalline ceramics. The corresponding flow stress increases with diminishing grain size of nanoceramics. The higher the temperature is, the smaller the flow stress is.

References

- Bobylev, S. V., Gutkin, M. Yu., Ovid'ko, I. A. (2008) Plastic deformation transfer through the amorphous intercrystallite phase in nanoceramics. *Physics of the Solid State*, 50 (10), 1888–1894. <https://doi.org/10.1134/S106378340810017X> (In English)

- Bobylev, S. V., Ovid'ko, I. A. (2008) Dislocation nucleation at amorphous intergrain boundaries in deformed nanoceramics. *Physics of the Solid State*, 50 (4), 642–648. <https://doi.org/10.1134/S1063783408040082> (In English)
- Chen, D., Zhang, X.-F., Ritchie, R. O. (2000) Effects of grain-boundary structure on the strength, toughness, and cyclic-fatigue properties of a monolithic silicon carbide. *Journal of the American Ceramic Society*, 83 (8), 2079–2081. <https://doi.org/10.1111/j.1151-2916.2000.tb01515.x> (In English)
- Clarke, D. R. (1979) On the detection of thin intergranular films by electron microscopy. *Ultramicroscopy*, 4 (1), 33–44. [https://doi.org/10.1016/0304-3991\(79\)90006-8](https://doi.org/10.1016/0304-3991(79)90006-8) (In English)
- Clarke, D. R. (1987) On the equilibrium thickness of intergranular glass phases in ceramic materials. *Journal of the American Ceramic Society*, 70 (1), 15–22. <https://doi.org/10.1111/j.1151-2916.1987.tb04846.x> (In English)
- Demkowicz, M. J., Argon, A. S. (2004) High-density liquidlike component facilitates plastic flow in a model amorphous silicon system. *Physical Review Letters*, 93 (2), article 025505. <https://doi.org/10.1103/PhysRevLett.93.025505> (In English)
- Demkowicz, M. J., Argon, A. S. (2005a) Autocatalytic avalanches of unit inelastic shearing events are the mechanism of plastic deformation in amorphous silicon. *Physical Review B*, 72 (24), article 245206. <https://doi.org/10.1103/PhysRevB.72.245206> (In English)
- Demkowicz, M. J., Argon, A. S. (2005b) Liquidlike atomic environments act as plasticity carriers in amorphous silicon. *Physical Review B*, 72 (24), article 245205. <https://doi.org/10.1103/PhysRevB.72.245205> (In English)
- Demkowicz, M. J., Argon, A. S., Farkas, D., Frary, M. (2007) Simulation of plasticity in nanocrystalline silicon. *Philosophical Magazine*, 87 (28), 4253–4271. <https://doi.org/10.1080/14786430701358715> (In English)
- Dufour, L.-C., Monty, C., Petot-Ervas, G. (eds.). (1989) *Surfaces and interfaces of ceramic materials*. Dordrecht; Boston; London: Kluwer Publ., 820 p. <https://www.doi.org/10.1007/978-94-009-1035-5> (In English)
- Glezer, A., Pozdnyakov, V. (1995) Structural mechanism of plastic deformation of nanomaterials with amorphous intergranular layers. *Nanostructured Materials*, 6 (5-8), 767–769. [https://doi.org/10.1016/0965-9773\(95\)00171-9](https://doi.org/10.1016/0965-9773(95)00171-9) (In English)
- Gutkin, M. Yu., Ovid'ko, I. A. (2009) Plastic flow in amorphous covalent solids and nanoceramics with amorphous intergranular layers. *Reviews on Advanced Materials Science*, 21 (2), 139–154. (In English)
- Gutkin, M. Yu., Ovid'ko, I. A. (2010a) A composite model of the plastic flow of amorphous covalent materials. *Physics of the Solid State*, 52 (1), 58–64. <https://doi.org/10.1134/S1063783410010105> (In English)
- Gutkin, M. Yu., Ovid'ko, I. A. (2010b) Plastic flow and fracture of amorphous intercrystalline layers in ceramic nanocomposites. *Physics of the Solid State*, 52 (4), 718–727. <https://doi.org/10.1134/S1063783410040086> (In English)
- Gutkin, M. Yu., Ovid'ko, I. A., Pande, C. S. (2004) Yield stress of nanocrystalline materials: Role of grain-boundary dislocations, triple junctions and Coble creep. *Philosophical Magazine*, 84 (9), 847–863. <https://doi.org/10.1080/14786430310001616063> (In English)
- Gutkin, M. Yu., Ovid'ko, I. A., Skiba, N. V. (2004) Emission of partial dislocations by grain boundaries in nanocrystalline metals. *Physics of the Solid State*, 46 (11), 2042–2052. <https://doi.org/10.1134/1.1825547> (In English)
- Hoffmann, M. J., Petzow, G. (eds.). (1994) *Tailoring of mechanical properties of Si₃N₄ ceramics*. Dordrecht: Springer Publ., 451 p. <https://www.doi.org/10.1007/978-94-011-0992-5> (In English)
- Hulbert, D. M., Jiang, D., Kuntz, J. D. et al. (2007) A low-temperature high-strain-rate formable nanocrystalline superplastic ceramic. *Scripta Materialia*, 56 (12), 1103–1106. <https://doi.org/10.1016/j.scriptamat.2007.02.003> (In English)
- Keblinski, P., Phillpot, S. R., Wolf, D. et al. (1996) Thermodynamic criterion for the stability of amorphous intergranular films in covalent materials. *Physical Review Letters*, 77 (14), 2965–2968. <https://doi.org/10.1103/PhysRevLett.77.2965> (In English)
- Keblinski, P., Phillpot, S. R., Wolf, D., Gleiter, H. (1997) Amorphous structure of grain boundaries and grain junctions in nanocrystalline silicon by molecular-dynamics simulation. *Acta Materialia*, 45 (3), 987–998. [https://doi.org/10.1016/S1359-6454\(96\)00236-4](https://doi.org/10.1016/S1359-6454(96)00236-4) (In English)
- Kleebe, H. J. (1997) Structure and chemistry of interfaces in Si₃N₄ ceramics studied by transmission electron microscopy. *Journal of the Ceramic Society of Japan*, 105 (1222), 453–475. <https://doi.org/10.2109/jcersj.105.453> (In English)
- Kleebe, H.-J., Cinibulk, M. K., Cannon, R. M., Rühle, M. (1993) Statistical analysis of the intergranular film thickness in silicon nitride ceramics. *Journal of the American Ceramic Society*, 76 (8), 1969–1977. <https://doi.org/10.1111/j.1151-2916.1993.tb08319.x> (In English)
- Kleebe, H. J., Hoffmann, M. J., Rühle, M. (1992) Influence of secondary phase chemistry on grain boundary film thickness in silicon nitride. *Zeitschrift für Metallkunde*, 83 (8), 610–617. (In English)
- Mo, Y. F., Szułfarska, I. (2007) Simultaneous enhancement of toughness, ductility, and strength of nanocrystalline ceramics at high strain-rates. *Applied Physics Letters*, 90 (18), article 181926. <https://doi.org/10.1063/1.2736652> (In English)

- Ovid'ko, I. A., Sheinerman, A. G. (2009) Enhanced ductility of nanomaterials through optimization of grain boundary sliding and diffusion processes. *Acta Materialia*, 57 (7), 2217–2228. <https://doi.org/10.1016/j.actamat.2009.01.030> (In English)
- Ovid'ko, I. A., Skiba, N. V., Sheinerman, A. G. (2008) Influence of grain boundary sliding on fracture toughness of nanocrystalline ceramics. *Physics of the Solid State*, 50 (7), 1261–1265. <https://doi.org/10.1134/S1063783408070123> (In English)
- Pozdnyakov, V. A., Glezer, A. M. (1995) Anomalies of Hall-Petch dependence for nanocrystalline materials. *Technical Physics Letters*, 21 (1), 31–36. (In English)
- Romanov, A. E., Vladimirov, V. I. (1992) Disclinations in crystalline solids. In: F. R. N. Nabarro (ed.). *Dislocations in solids. Vol. 9*. Amsterdam; London; New York: North-Holland Publ., pp. 191–402. (In English)
- Subramaniam, A., Koch, C. T., Cannon, R. M., Rühle, M. (2006) Intergranular glassy films: An overview. *Materials Science and Engineering A*, 422 (1-2), 3–18. <https://doi.org/10.1016/j.msea.2006.01.004> (In English)
- Szlufarska, I., Nakano, A., Vashishta, P. (2005) A crossover in the mechanical response of nanocrystalline ceramics. *Science*, 309 (5736), 911–914. <https://doi.org/10.1126/science.1114411> (In English)
- Tomsia, A. P., Glaeser, A. M. (eds.). (1998) *Ceramic microstructures: Control at the atomic level*. Boston: Springer Publ., 854 p. <https://www.doi.org/10.1007/978-1-4615-5393-9> (In English)
- Xu, X., Nishimura, T., Hirosaki, N. et al. (2006) Superplastic deformation of nano-sized silicon nitride ceramics. *Acta Materialia*, 54 (1), 255–262. <https://doi.org/10.1016/j.actamat.2005.09.005> (In English)
- Zhang, Z. L., Sigle, W., Koch, C. T. et al. (2011) Dynamic behavior of nanometer-scale amorphous intergranular film in silicon nitride by *in situ* high-resolution transmission electron microscopy. *Journal of the European Ceramic Society*, 31 (9), 1835–1840. <https://doi.org/10.1016/j.jeurceramsoc.2011.03.016> (In English)